VTT Technical Research Centre of Finland

Experimental comparison of regeneration methods for CO2 concentration from air using amine-based adsorbent

Elfving, Jere; Kauppinen, Juho; Jegoroff, Mikko; Ruuskanen, Vesa; Järvinen, Lauri; Sainio, Tuomo

Published in:
Chemical Engineering Journal

DOI:
10.1016/j.cej.2020.126337

Published: 15/01/2021

Document Version
Publisher's final version

Chemical Engineering Journal 404 (2021) 126337

Contents lists available at ScienceDirect

Chemical Engineering Journal

journal homepage: www.elsevier.com/locate/cej

Experimental comparison of regeneration methods for CO_2 concentration from air using amine-based adsorbent

Jere Elfving[a,*], Juho Kauppinen[a], Mikko Jegoroff[a], Vesa Ruuskanen[b], Lauri Järvinen[b], Tuomo Sainio[c]

[a] VTT Technical Research Centre of Finland Ltd., Koivurannantie 1, FI-40101 Jyväskylä, Finland
[b] Lappeenranta-Lahti University of Technology, School of Energy Systems, Skinnarilankatu 34, FI-53850 Lappeenranta, Finland
[c] Lappeenranta-Lahti University of Technology, School of Engineering Science, Skinnarilankatu 34, FI-53850 Lappeenranta, Finland

HIGHLIGHTS

- Only 60 °C coupled with purge gas regenerates amine-based adsorbent by over 85%.
- Coupling purge gas with TVSA is beneficial in terms of CO_2 productivity.
- TVSA with purge gas can have lower specific energy requirement than closed TVSA.
- Using air and 100 °C during regeneration significantly decreases adsorbent capacity.
- Mild temperature TVSA with purge gas is a viable direct air capture process option.

GRAPHICAL ABSTRACT

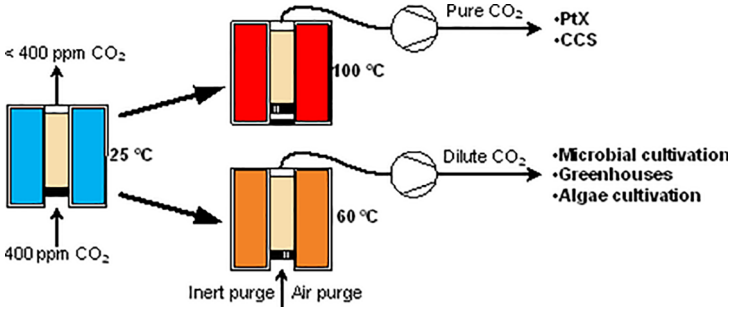

ARTICLE INFO

Keywords:
Direct air capture
CO_2 adsorption
Adsorbent regeneration
Working capacity
Specific energy requirement
Regenerability

ABSTRACT

Comparison of different regeneration options for direct air capture (DAC) has usually been limited to only consider pure CO_2 production, limiting the process options to e.g. temperature-vacuum swing adsorption (TVSA) or steam-stripping. In this work, detailed experimental comparison is conducted of temperature swing adsorption (TSA/TCSA) and TVSA for DAC. Particularly, TVSA is assessed with air or inert gas purge flow (TVCSA) and without purge flow. The working capacity, regeneration specific energy requirement (SER) and adsorbent regenerability of these processes was compared. For all other studied regeneration options except TVSA without purge flow, over 85% regeneration was obtained already at 60 °C. Isobaric TSA at 60 °C had the lowest regeneration SER of 4.2 MJ/kg_{CO2}. Coupling TSA with mild vacuum improved desorption rate and increased working capacity from 0.47 to 0.51 $mmol_{CO2}/g_{sorbent}$, requiring 7.5 MJ/kg_{CO2} for regeneration. Without purge flow, TVSA resulted in only 0.39 $mmol_{CO2}/g_{sorbent}$ with the SER of 8.6 MJ/kg_{CO2} at 100 °C. Due to lower allowable regeneration temperature of 60 °C, mild vacuum TVSA with air flow also had a lower cyclic capacity decrease rate of 0.26%/cycle compared to 0.38%/cycle with TVSA without purge flow at 100 °C. However, using 100 °C with air flow in the TVSA process lead to a significant capacity decrease of 0.6%/cycle. Therefore, using either air or inert purge flow below 100 °C coupled with mild vacuum has benefits over the TVSA process with no inflow in terms of CO_2 productivity, specific energy requirement and adsorbent regenerability. For utilization purposes that require low-concentration CO_2, TVSA with purge flow should thus be considered as a viable regeneration option for direct air capture along with isobaric TSA.

* Corresponding author.
E-mail address: jere.elfving@vtt.fi (J. Elfving).

https://doi.org/10.1016/j.cej.2020.126337
Received 28 May 2020; Received in revised form 14 July 2020; Accepted 16 July 2020
Available online 22 July 2020

1. Introduction

For carbon capture and storage (CCS) or utilization (CCU) purposes, CO_2 capture from flue gases or air has been proposed using various technologies. Aqueous amine solvent-based post-combustion capture (PCC) is a relatively mature technology, but suffers from high heat demand related to the regeneration of the solvent [1,2]. Also, PCC processes based on primary and secondary amines such as monoethanolamine (MEA) may emit amine degradation compounds that are toxic and carcinogenic [3]. Therefore, alternatives such as amino acid salt solutions have been proposed as a more environmentally friendly option to conventional amines [4]. NaOH-based process was the first process type suggested for direct air capture (DAC) [5]. This approach was deemed as highly energy-intensive [6], although pilot-scale results have shown better results for the process type using KOH-solution than the early techno-economic analysis in terms of energy requirement [7]. As an alternative to solvent-based processes, solid adsorbents have been widely studied for both PCC [8–10] and DAC [11]. Solid adsorbent-based DAC has several advantages over the solvent-based solutions such as small unit size and scalability [12], low temperature requirement of usually less than 100 °C [11,13] and fairly simple design, while still being able to produce almost pure CO_2 [11,13].

While physical adsorbents such as activated carbons and metal–organic frameworks (MOF) are reasonable to use in PCC [8,10,14], in DAC they are usually not selective enough, and amine-functionalization of the porous structure is required to obtain higher capacities for the resulting adsorbent [11,15]. CO_2 adsorption capacities for amine-impregnated and amine-grafted adsorbents in PCC conditions (10–15% CO_2) are in the range of 2–5 $mmol_{CO2}/g_{sorbent}$ and below 3 $mmol_{CO2}/g_{sorbent}$, respectively [8]. In DAC conditions, amine-impregnated adsorbents usually have 1–2 $mmol_{CO2}/g_{sorbent}$, while for amine-grafted materials the capacities range from 0.1 to even over 2 $mmol_{CO2}/g_{sorbent}$ [11]. However, even higher capacities have been obtained in both PCC and DAC conditions, such as 11.8 $mmol_{CO2}/g_{sorbent}$ for a mesoporous silica functionalized by surface-initiated amine polymerization from humid 8% CO_2 [16] and 3.89 $mmol_{CO2}/g_{sorbent}$ from dry 400 ppm CO_2 for a MOF functionalized with diamines [17]. While a higher CO_2 concentration in PCC leads to higher CO_2 capacities compared to DAC conditions, the difference is not always significant for amine-based adsorbents. For example, a commercial aminoresin Lewatit VP OC 1065 shows fairly steep improvements as a function of CO_2 concentration, having a CO_2 adsorption capacity of 1.06 $mmol_{CO2}/g_{sorbent}$ from 400 ppm CO_2, 1.64 $mmol_{CO2}/g_{sorbent}$ from 5000 ppm CO_2 at 20 °C [18] and 2.6 $mmol_{CO2}/g_{sorbent}$ from 40% CO_2 at 40 °C [19]. However, Lee et al. [20] reported the CO_2 capacities of a diamine-functionalized MOF in dry DAC (0.39 mbar CO_2) and PCC conditions (0.15 bar CO_2) fairly close to each other, being 2.83 and 3.62 $mmol_{CO2}/g_{sorbent}$, respectively. The adsorption capacity of the proprietary aminoresin used in this study has been measured in earlier work [21] to be 0.54 $mmol_{CO2}/g_{sorbent}$ in dry DAC conditions and 0.89 $mmol_{CO2}/g_{sorbent}$ in humid conditions at 25 °C. It is therefore in the lower end of the reported materials capacity-wise, but is fairly comparable to amine-grafted adsorbents.

Equally important to obtaining a high CO_2 adsorption capacity is regeneration of the adsorbent. One of the most important goals in the regeneration is to maximize CO_2 working capacity, since with low CO_2 capacity the allowable cost of adsorbent drops unrealistically low, making the whole process economically infeasible [22]. While pressure swing adsorption (PSA) may be a viable regeneration option for PCC [10], in DAC this method cannot be used without extensive compression of air or unpractically low vacuum levels [21,23]. Temperature swing adsorption (TSA) is often the method for regeneration of amine-based CO_2 adsorbents in laboratory-scale studies [11]. This method is simple in design, but the disadvantages are that the product CO_2 is diluted and significant oxidative degradation of amine can take place at desorption temperatures slightly above 100 °C [24]. To counter the oxidative degradation, inert gas can be used instead of air, which can be costly in process scale. An option for using TSA for high-purity CO_2 production is to use pure CO_2 as stripping gas, but in this approach the risk is adsorbent deactivation via urea formation [25,26]. Also, because desorption takes place in a high-concentration CO_2 atmosphere, the working capacity is reduced. A derivative of TSA is steam-stripping, in which saturated steam is used as the inert gas purge and high-purity CO_2 can be produced if water is condensed from the product gas [18,27]. However, a significant drawback in this process is adsorbent deactivation via leaching of the amines [28,29]. This process can also be coupled with vacuum to enhance desorption rate and produce steam at lower than 100 °C temperatures, but leaching of amines by steam remains a problem [30].

Temperature-vacuum swing adsorption (TVSA) process uses coupled vacuum and temperature swing for desorption of CO_2, and can be used to produce near 100% CO_2 from air [13,31]. However, this process reduces the attainable CO_2 working capacity and increases required temperature swing compared to TCSA or TSA [21,23]. This is because in the TVSA process the inlet is closed during desorption to prevent product dilution, which leads to desorption taking place in high-concentration CO_2 atmosphere when CO_2 is produced into the adsorption chamber and the vacuum pump [13,23]. For example, Wurzbacher et al. [23] produced 0.44 $mmol_{CO2}/g_{sorbent}$ using TCSA at 90 °C, while using TVSA only produced 0.27 $mmol_{CO2}/g_{sorbent}$ with 50 mbar vacuum at 90 °C. With a pilot-scale DAC device using TVSA process, Bajamundi et al. [13] produced only 3.4 kg CO_2 at 80 °C from over 5.6 kg of the CO_2 adsorbed on the aminoresin beds in the best case. Increasing the desorption temperature may help increase the working capacity, but increases energy requirement and the risk of adsorbent thermal degradation. Based on CO_2 isotherms [21], another option for increasing working capacity is to couple air or inert gas flow simultaneously with the TVSA process. Using TVSA coupled with air or inert gas purge has not been proposed for DAC, probably due to assumed high energy requirements of vacuuming and lowered product purity. TVSA with inert gas purge has been compared to steam stripping with vacuum as a regeneration method for DAC in terms of desorption rate [30], but the energy requirement or adsorbent regenerability using this process has not been compared to other options to the authors' best knowledge.

Along with the specific energy requirement and daily working capacity, adsorbent regenerability is one of the most important economic factors of the cyclic DAC process [22]. However, in testing the regenerability of amine-based adsorbents for PCC or DAC applications, cyclic experiments have usually been done with less than 20 cycles [25]. Especially in DAC studies cyclic experiments have been limited with usually less than 10 cycles [32,33], although in some papers over 20 cycles [34] or even 100 cycles [35] have been conducted. From only a few cycles it is hard to deduce anything about the long-term stability of the adsorbent, especially if the uncertainty of the method has not been reported. The long-term regenerability should also be compared between different regeneration options, but the studies comparing regeneration conditions have mainly focused only on degradation mechanisms [19,25,36]. Little to no comparison has been made on the trends of cyclic CO_2 adsorption and desorption capacities in over 20 cycles using different regeneration processes.

Different CO_2 utilization purposes require different CO_2 purities and therefore different DAC process types. High purity of the produced CO_2 is especially important for CO_2 utilization in e.g. Fischer-Tropsch process [37], and may thus require processes such as TVSA. However, many CO_2 utilization purposes exist where there is no need to supply near 100% CO_2, such as greenhouses and microbial and algae cultivation for food or fuels. In greenhouses and especially in closed ones, CO_2 supply is required to not let the CO_2 concentration decrease and reduce plant growth [38]. The use of DAC for greenhouses has been proposed earlier by the use of low-capacity sorbents such as zeolite 13X [39] and alkali metal carbonates [40,41]. Another low-concentration application where DAC has been proposed and tested is microalgae cultivation, in

which Brilman et al. [42] found optimal growth in CO_2 concentration of only 1.5–2%. Also, DAC has been used to supply CO_2 for microbial cultivation to produce edible protein in the Neo-Carbon Food project [43], although the optimal CO_2 concentration for the cultivated microbes is as of yet unknown. With 40–60% capture ratio that is a realistic range for adsorbent based DAC [13], Wilcox et al. [44] estimated the work of separation to rise e.g. from less than around 200 kJ/mol_{CO2} (4.5 MJ/kg_{CO2}) to over 550–700 kJ/mol_{CO2} (12.5–15.9 MJ/kg_{CO2}) with produced CO_2 purities less than 5% and over 90%, respectively. Thus, these results hint that to lower the cost of DAC, the process should be tailored in terms of required CO_2 purity for each purpose. This requires detailed comparison of all the available regeneration methods and not just the process options that aim to produce pure CO_2.

In this work, an automated and modifiable fixed-bed adsorption–desorption device is used for studying the regeneration options for DAC using temperature-swing adsorption (TSA) and temperature-vacuum swing adsorption (TVSA) processes with and without inlet flow. The purpose of this analysis is to assess whether using regeneration methods with inlet flow such as TSA, leading to low-purity CO_2, show significant working capacity or specific energy requirement benefits compared to the TVSA process without inlet flow during regeneration. Also, combining purge flow such as air or inert gas with the TVSA process is assessed here in DAC conditions using an amine-based adsorbent. Evaluating such process for DAC with amine-based adsorbent using dry air as the purge gas is done here for the first time to the authors' best knowledge. First, the pseudo-equilibrium working capacities are compared for all selected experimental conditions. Then, the working capacity dynamics of these processes are compared, followed by a preliminary assessment of the specific energy requirements. Finally, the progress of cyclic adsorption and desorption capacities are studied over multiple experimental cycles for TCSA and TVSA processes to see the effect of different process options on the regenerability of the amine-based adsorbent.

2. Experimental and calculation methods

2.1. Fixed-bed CO_2 adsorption–desorption setup

The experimental setup used in this study was designed and built in VTT. Schematic of the experimental setup is shown in Fig. 1. The setup has five Bronkhorst mass-flow controllers (MFCs) to reach the wanted inlet gas composition. MFCs 1–3 are mainly used for inert purging gas or air, whereas MFCs 4–5 are mainly used for 100% CO_2, mixtures of CO_2 or air. Fig. 1 shows two different inlet routes to the adsorption column as well as a column bypass route, which are needed e.g. when having to purge the column with N_2 from MFC 1 or 2 while measuring the inlet concentration fed through the column bypass route. Optionally, the inlet gas through inlet route 2 can be humidified, although in this study only dry experiments were done. The inlet gas flow is then led to the adsorption column with two thermocouples. Pressure measurements are located before and after the column. Safety valves are also located before and after the column for the instance of pressure reaching over 6 bar. After the column, the gas flow can be directed through vacuum (< 1 bar) route or overpressure (1–5 bar) route. The total pressure over both routes is controlled by separate Flowserve Kämmer pressure control valves either via manual set-point or using the pressure measurement after the column for PID control. At the outlet there are measurements for gas flow rate, humidity, pressure and ppm- and %-scale measurements of CO_2 concentration. All gas flow movements are controlled by 2-way or 3-way magnetic valves.

Fig. 2 shows the structure of the adsorption column, dimensions of the sample chamber and places of the thermocouples. The adsorption column is practically a steel pipe surrounded by a steel jacket, in which cooling or heating liquid flows. The adsorbent sample is placed on the top of a sieve welded into the column and fixed from top by placing quartz wool between the sample and a sieve that is attached to the thermocouple. Temperature of the sample is measured radially from the middle of the sample and axially 10 mm above the lower sieve. Thus, the tip of the thermocouple inside the adsorption column is

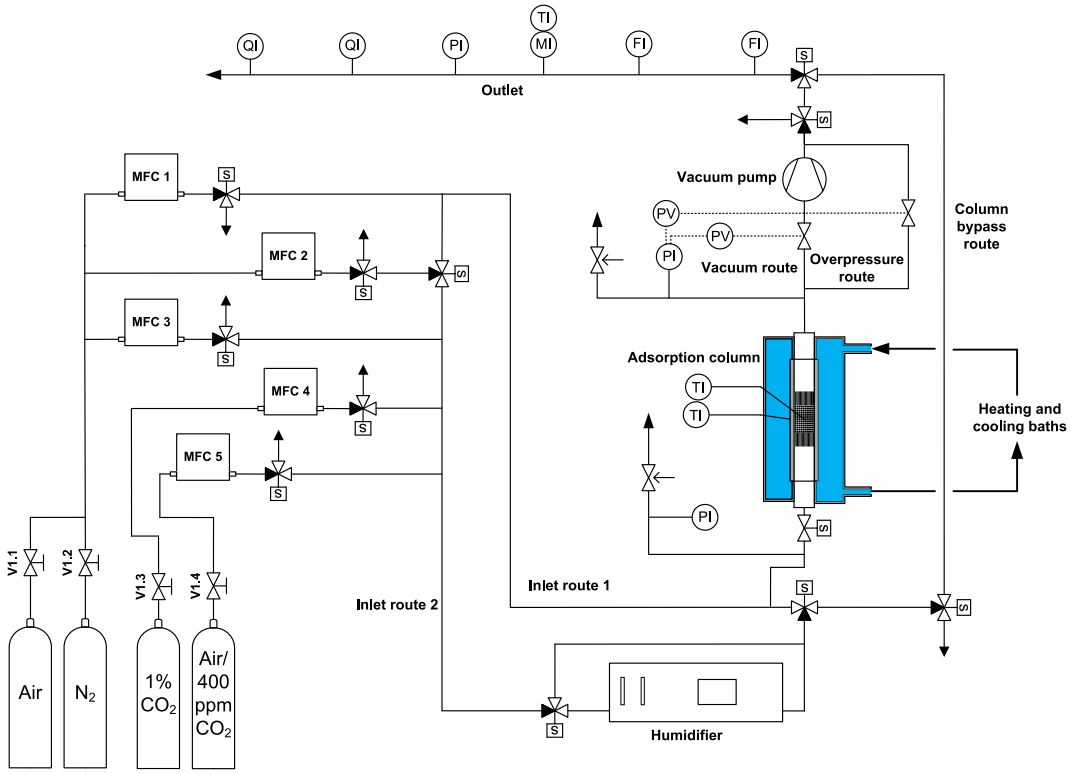

Fig. 1. Experimental setup for fixed-bed adsorption and desorption of CO_2.

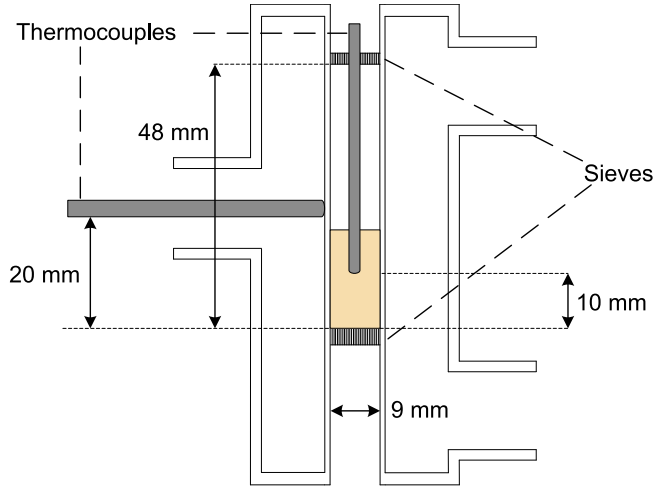

Fig. 2. The adsorption column. The sample in the figure represents volume of 0.5 g of the studied resin.

approximately ½ and ¼ from the bottom of the adsorbent for 0.5 g and 1 g samples of the aminoresin used in this study, respectively. Also, temperature is measured from the outer wall of the column 20 mm above the lower sieve. Temperature of the sample is controlled by leading hot or cool liquid to the jacket surrounding the column. For this purpose, separate hot and cool liquid circulations are controlled by two Julabo Corio CD 200F refrigerated/heating circulators. The pass of either cool or hot liquid to the jacket is controlled by 2-way magnetic valves. Currently the operable temperature range is between −10 °C and 105 °C.

All magnetic valves, MFCs, pressure control valves and the vacuum pump are controlled via a LabVIEW-based control and data acquisition program. The program was developed in co-operation between VTT and LUT School of Energy Systems. The program is capable of manual control as well as user-built automatic stepwise sequences. The sequences are built as a spreadsheet that is fed to the program at the start of the experimental run. Each step is run until a fixed time determined in the spreadsheet. The sequence-based control allows to perfectly reproduce the experimental cycles, saves time and resources, and allows to conveniently run continuous cyclic adsorption/desorption. Data sampling rate was 0.5 Hz. Lists of the main components and dimensions of the experimental setup can be found in Supplementary data.

2.2. CO_2 adsorption–desorption experiments

The adsorbent used in this study is a proprietary aminoresin, the characterization of which has been reported earlier in Elfving et al. [45]. In this work, the adsorbent was pre-dried in air at 90 °C. Typically, 0.5 g or 1 g of pre-dried adsorbent was weighed and fixed into the adsorption column with 0.04 g of silica wool below sieve and above the adsorbent. The pre-dried resin had a bulk density of approximately 0.45 g/ml and therefore the sample batch sizes correspond to volumes of 1.1 ml and 2.2 ml. The lower mass was used in cyclic experiments. For other experiments, to achieve higher dynamic responses during desorption i.e. higher CO_2 concentration and flow-rate peaks, 1 g of adsorbent was used, in which case the sample chamber was almost full. The pre-dried adsorbent still had CO_2 and H_2O adsorbed from air, and in this work these are referred to as pre-adsorbed species.

All experiments were designed beforehand and then run on the sequence-based control in LabVIEW. Because this study focuses on regeneration, the adsorption phase was kept constant in all experimental runs, using 1000 ml/min total flow rate of approximately 400 ppm CO_2 mixed using 1% CO_2 with purities of 3.5 CO_2 and 5.0 N_2, and 5.0 nitrogen at 25 °C. For regeneration, different conditions were used based on each process. The regeneration processes were divided into four steps: 1) 'Purge 1' consisting of concentration swing to 0 ppm CO_2 in TCSA coupled with vacuuming in TVCSA, or only vacuuming in TVSA; 2) temperature swing to 60 °C ('TS 1'); 3) temperature swing to 100 °C ('TS 2'); 4) concentration swing to 0 ppm CO_2 for TSA and TVSA processes ('Purge 2'). In TVSA processes with inlet flow, 'Purge 1', 'TS 1' and 'TS 2' were conducted using 400 ppm CO_2. The TVSA process without inlet flow is referred to as "closed TVSA" in this work. Step times were fixed to enable comparison between process steps. The different processes and steps involved are illustrated in Table 1.

For regeneration processes targeting equilibrium or pseudo-equilibrium CO_2 capacities, 1000 ml/min flow rate was used. For studying dynamics more closely, 40 ml/min was chosen as a compromise between fast measurement response and process-relevant flow rate to adsorbent mass ratio. Used vacuum levels were 500 mbar representing a mild-vacuum process, and the minimum achievable at the given flow rate, being 200 mbar with 1000 ml/min and 25 mbar with 40 ml/min. Used inlet gas was either N_2 for concentration swing, 400 ppm CO_2 mixed similarly as in the adsorption phase for 1000 ml/min flow or premixed 400 ppm CO_2 for 40 ml/min flow. Also, compressed dry air with approximately 400 ppm CO_2 was used in the cyclic experiments to find the effect of oxygen on regenerability.

2.3. Calculation of capacities

Here the CO_2 capacities are represented as mmol per gram of dry activated adsorbent, using the mass of pre-adsorbed species (CO_2, H_2O) in each sample to correct the pre-dried sample mass. The mass of pre-adsorbed species was calculated by measuring the CO_2 and H_2O concentrations leaving the sample during initial regeneration phase with 1000 ml/min N_2 flow and heating to 100 °C before the actual experimental cycle. The same procedure was also done without sample, but the resulting masses were negligible, being mainly the contribution of air inside the experimental setup column and lines. The contribution of pre-adsorbed species of the pre-dried sample measured this way was 1.4–2.5 w-%.

Typically, the capacities were calculated based on integration of the CO_2 concentration and flow rate [21,23]. The CO_2 concentration was pressure- and temperature corrected to SATP-conditions (see Supplementary data). The capacities in the desorption phase were constructed of capacities calculated using ppm-scale measurements when under 5000 ppm, and %-scale measurements when over 5000 ppm. Typically this meant that combination of ppm and %-scale

Table 1
Experimental CO_2 adsorption/desorption processes and step changes. Total inlet gas flow rate was 40 or 1000 ml/min during all phases, except for TVSA closed. For TVSA closed, inlet flow during 'Purge 2' was 1000 ml/min.

Process	Adsorption	Time	Purge 1	Time	TS 1	Time	TS 2	Time	Purge 2	Time
TSA	400 ppm CO_2, 25 °C	2 h	–	–	60 °C	1 h	100 °C	1 h	0 ppm CO_2	> 0.5 h
TCSA	400 ppm CO_2, 25 °C	2 h	0 ppm CO_2	0.5 h	60 °C	1 h	100 °C	1.5 h	–	–
TVSA	400 ppm CO_2, 25 °C	2 h	400 ppm CO_2, vacuum	0.5 h	60 °C	1 h	100 °C	1/1.5 h*	0 ppm CO_2	> 0.5 h
TVCSA	400 ppm CO_2, 25 °C	2 h	0 ppm CO_2, vacuum	0.5 h	60 °C	1 h	100 °C	1/1.5 h*	–	–
TVSA closed	400 ppm CO_2, 25 °C	2 h	No inflow, vacuum	0.5 h	60 °C	1 h	100 °C	1 h	0 ppm CO_2	> 0.5 h

* 1 h or 1.5 h for 1000 or 40 ml/min experiments, respectively.

results were used when inlet flow was 40 ml/min in regeneration phase, while only ppm-scale results were used in case of 1000 ml/min flow. Consequently, the results with only 1000 ml/min flow are more accurate than the 40 ml/min results, due to higher uncertainty of the %-scale sensor (< 0.25% ± 5% reading) vs. the ppm-scale sensor (± 5 ppm CO_2 + 2% reading). Dynamic profiles of both sensors in a 40 ml/min case along with other relevant variable profiles can be found in the Supplementary data.

Instead of measured inlet concentration like in Elfving et al. [21], in this work the inlet concentration was in the form of a step function. In adsorption phase and in desorption with 400 ppm CO_2 inlet flow, the step function value was calculated as a mean value of the concentration of the inlet gas when bypassing the column. Otherwise the step function was set to zero. This is an acceptable approximation, because the effect of dispersion was found to be small, which is shown in a typical experimental cycle in the Supplementary data. However, to gain the most accurate capacity values, the "empty column capacity", was subtracted from the pseudo-equilibrium and cyclic capacities presented in this work. For the dynamic capacity and specific energy requirement profiles in chapter 3.2, no such correction was used due to very small effect on the final capacity, typically less than 1%.

In closed TVSA runs the calculation was based on only integrating the volume flow rate instead of both volume and concentration due to practical reasons. Due to high amount of vacuumed total volume of about 81 ml compared to the less than 10 ml of produced CO_2, the produced CO_2 was generated between the adsorption column and the outlet of the vacuum pump. Therefore, no CO_2 was detected in the measurements during this vacuuming stage. The CO_2 capacity of the TVS phase was thus calculated based on the detected flow rate pulse, assuming the pulse detected in the flow-meter is nitrogen. Determination of experimental uncertainty in the calculation of capacities can be found in Supplementary data.

2.4. Calculation of regeneration specific energy requirements

The specific energy requirements calculated in this work are optimal numbers that are based on the experimental dynamic profiles of capacity, temperature, flow rate and vacuum pressure during regeneration phase. The specific energy requirement (SER) at each time point represents the cumulative specific energy requirement calculated based on the experimental vacuum level and temperature at that point, total gas volume flowed until that point, and the desorption CO_2 capacity acquired until that point. The SER values calculated in this work are ideal, and consider no energy losses. The energy requirement of the regeneration phase was calculated by:

$$E_{reg,tot} = E_{fan} + E_{s,a} + E_{s,CO2} + E_{des,CO2} + E_{vac} \quad (1)$$

where $E_{reg,tot}$ is the total energy requirement of the regeneration phase, divided into E_{fan}, $E_{s,a}$, $E_{s,CO2}$, $E_{des,CO2}$ and E_{vac}, which are the energy requirement contributions of air blowers, sensible heat of the adsorbent, sensible heat of adsorbed CO_2, desorption enthalpy of CO_2 and vacuum, respectively.

The fan energy required to blow air was calculated according to:

$$E_{fan} = \int \Delta p\, \dot{V}_{tot}\, dt \quad (2)$$

where Δp is the pressure drop along the adsorbent bed and $\dot{V}_{tot}$ is the total flow rate. Pressure drop over the adsorbent bed was here calculated using the Ergun equation:

$$\Delta p = \frac{150\,\mu\, L_{bed}\,(1-\varepsilon)^2 v_s}{{d_p}^2 \varepsilon^3} + \frac{1.75\, L_{bed}\, \rho_g (1-\varepsilon) {v_s}^2}{d_p\, \varepsilon^3} \quad (3)$$

where μ is the dynamic viscosity, L_{bed} is the length of the adsorbent bed, ε is the bed porosity, v_s is the superficial velocity of the gas, d_p is the adsorbent particle size and ρ_g is the gas density [46]. Sensible heat of dry adsorbent was calculated according to:

$$E_{s,a} = m_a\, c_{p,a}\, \Delta T \quad (4)$$

where m_a is the mass of adsorbent sample, $c_{p,a}$ is the specific heat capacity of the adsorbent, ΔT is the temperature difference in the temperature swing. Similarly, the sensible heat of desorbed CO_2 could be calculated as:

$$E_{s,CO2} = m_{CO2}\, c_{p,CO2}\, \Delta T \quad (5)$$

where m_{CO2} is the mass of desorbed CO_2, $c_{p,CO2}$ is the specific heat capacity of CO_2. However, the sensible heat of desorbed CO_2 was negligible in the calculations. The desorption heat of CO_2 was calculated using:

$$E_{des,CO2} = \int \Delta H\, \dot{n}_{CO2}\, dt \quad (6)$$

where ΔH is the CO_2 desorption enthalpy, $\dot{n}_{CO2}$is the molar flow rate of CO_2. The energy of the vacuum pump was calculated based on isothermal and irreversible work equation according to [47]:

$$E_{vac} = -P_{out} \int \dot{V}_{tot}\, dt \left(\frac{P_1}{P_{out}} - \frac{P_2}{P_{out}} + \ln\left(\frac{P_2}{P_1}\right) \right) \quad (7)$$

where P_{out} is the mean outlet (ambient) pressure during regeneration, P_1 is the pressure before vacuuming and P_2 is the vacuum pressure at given time point, measured after the column. To gain the specific energy requirements, the total energy requirement in Eq. (1) was then

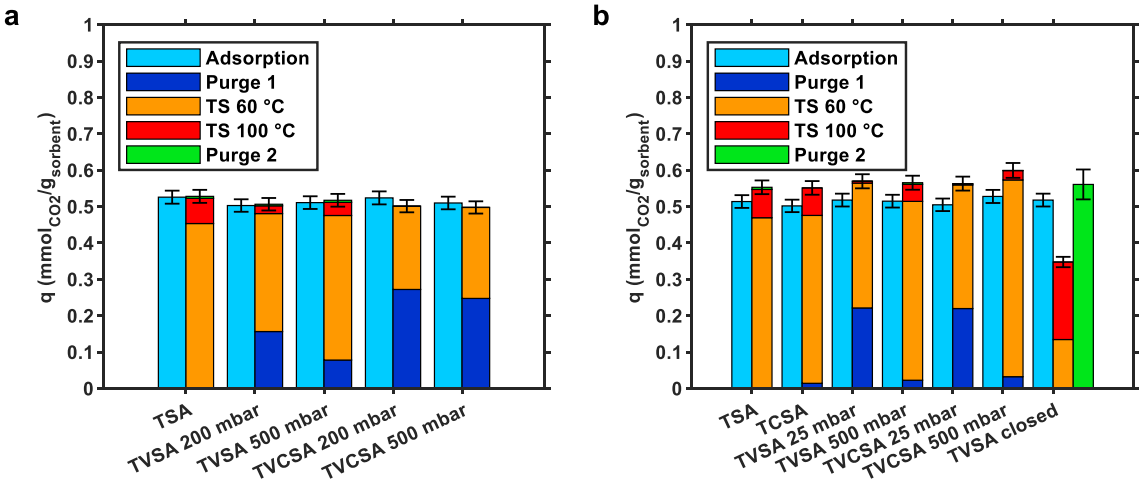

Fig. 3. Adsorption and desorption CO_2 capacities using a) 1000 ml/min; b) 40 ml/min total flow rate in desorption phase. 'Purge 2' in TVSA closed resulted from using N_2 purge after the closed TVS step with 1000 ml/min total flow rate. Error bars show the uncertainty.

divided by the produced mass of CO_2 in given experiment. A table with values and/or the source of each constant and variable used for the energy requirement calculations is supplied in the Supplementary data.

3. Results & discussion

3.1. Working capacity comparison

As described in chapter 2.2, adsorption of 400 ppm CO_2 was followed by a stepwise regeneration of the adsorbent. Fig. 3 shows the attained working capacities after each step in the studied regeneration processes. The adsorption capacities are within 0.50–0.53 $mmol_{CO2}/g_{sorbent}$. Comparison of Fig. 3b with Fig. 3a shows that the desorption capacities in the runs with 40 ml/min inlet flow are slightly higher than those with 1000 ml/min inlet flow. This difference originates from the different method of capacity calculation in the 40 ml/min results compared to 1000 ml/min results (see chapter 2.3). The total desorption capacities in 1000 ml/min and 40 ml/min cases are in the range of 0.50–0.53 $mmol_{CO2}/g_{sorbent}$ and 0.55–0.60 $mmol_{CO2}/g_{sorbent}$, respectively. Because the total desorption capacities are equal or higher than the adsorption capacities with uncertainty taken into account, regeneration of the adsorbent was complete after each 4-step regeneration process.

Fig. 3a shows that the effect of vacuum level on the initial purge step working capacity is larger for TVSA than for TVCSA in regeneration with 1000 ml/min flow rate. This is an expected result in that the partial pressure of CO_2 for TVCSA is zero with both vacuum levels. In the regeneration experiments with 40 ml/min flow rate, the vacuum level differences were higher. Consequently, Fig. 3b shows much bigger differences in initial purge working capacities between the two vacuum levels compared to Fig. 3a. On the other hand, the equilibrium state in terms of CO_2 partial pressure is still the same in the TVCSA experiments, although the vacuum level is different. The differences in the purge capacities between the two vacuum levels, especially with the lower flow rate, mainly originate from dynamics, since the first step was not carried out until equilibrium.

It is notable that the working capacities are mostly above 90% of the total desorption capacity already with 60 °C temperature swing. Especially in the case of TVCSA with 1000 ml/min inlet flow only negligible desorption was observed at 100 °C. As expected, the largest working capacity differences between 60 °C and 100 °C temperature swing are for TSA, TCSA and closed TVSA cases. However, even for TSA the working capacities at 60 °C are already 85% and 86% of the total desorption capacity using 40 and 1000 ml/min flow rate during desorption, respectively. However, for closed TVSA the effect of temperature increase from 60 °C to 100 °C is notable, with only 0.13 $mmol_{CO2}/g_{sorbent}$ being released at 60 °C. Also, the total desorption capacity released during TVS with closed inlet is only 0.35 $mmol_{CO2}/g_{sorbent}$, that is considerably lower than in any of the experiments with inlet flow. Total desorption capacity of 0.56 $mmol_{CO2}/g_{sorbent}$ in the closed TVSA experiment was obtained when opening the column inlet to nitrogen purge.

The desorption capacity results show that even 60 °C can be used for regeneration with no significant decrease of working capacity compared to 100 °C when using inert purge or 400 ppm CO_2 flow. The result is in line with other studies showing that air [48] or purge flow such as steam under vacuum [30] can be used to fully regenerate amine-based adsorbents even below 100 °C. However, although lower desorption temperatures may be enough to fully regenerate the adsorbent with plenty of time, kinetics may be slowed significantly. Also, possible benefits of coupling vacuum and purging flow during temperature swing steps seem to be minor if only comparing the final working capacities. Therefore, the experimental dynamic capacity profiles are presented below to broaden this comparison to the differences in dynamics. The runs with 1000 ml/min inlet flow in desorption are not discussed in terms of dynamics because the flow rate per mass of adsorbent ratio is too high considering process scale.

3.2. Dynamic capacity profiles

Fig. 4a shows that in TSA regeneration the production of working capacity is delayed at first, taking about 4 min before the capacity starts to increase. This delay could be attributed to three factors: 1) heat transfer from the jacket through the steel wall and into the adsorbent; 2) time spent for the flow to reach the concentration measurements and; 3) CO_2 concentration measurement sensor response time. After this initial period the capacity starts to rise quickly, but slows down eventually, showing that equilibrium state was not reached within 1 h of heating. Fig. 4b shows that the trend for TCSA is very similar to TSA, except for the start where an almost insignificant amount of CO_2 is removed by cool N_2 purge alone. Therefore, probably even slightly higher capacities are obtainable for TSA/TCSA already at 60 °C. However, the desorption rates at 60 °C are much slower than at 100 °C. Increasing the temperature to 100 °C quickly increases the working capacities from 0.47 and 0.48 to maximum values of 0.55 and 0.56 $mmol_{CO2}/g_{sorbent}$ for TSA and TCSA, respectively. Second purge in TSA increases the working capacity to the same as in TCSA, 0.56 $mmol_{CO2}/g_{sorbent}$. Similar type behavior was reported by Goeppert et al. [48] for a fumed silica-PEI adsorbent, who found that only 12–14% of the adsorption capacity at 25 °C was left at 65 °C. On the other hand, they also reported significantly reduced desorption kinetics below 85 °C, especially at 50–60 °C.

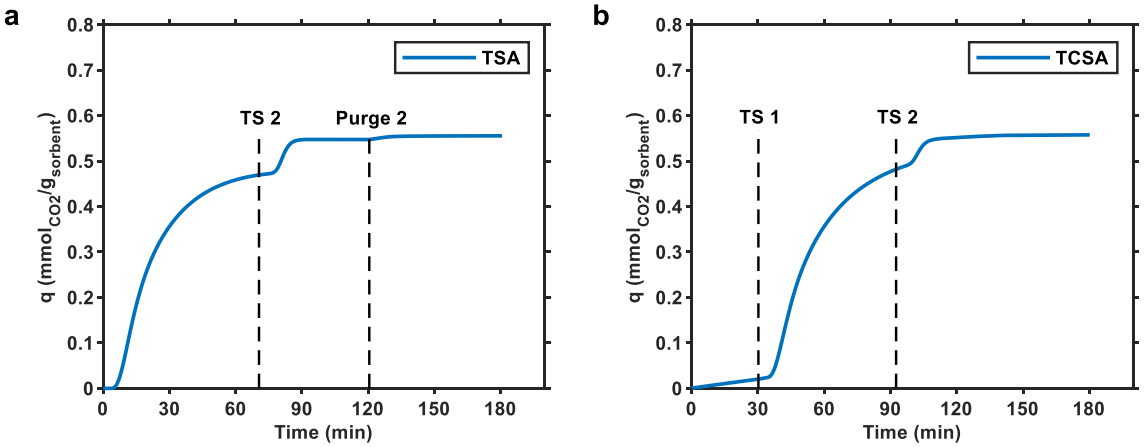

Fig. 4. Desorption capacity profiles using 40 ml/min flow of a) 400 ppm CO_2; b) 0 ppm CO_2. Temperature of the adsorbent was set to 60 °C a) at start; b) after 'TS 1' and to 100 °C after 'TS 2'. 'Purge 2' refers to switching flow from 400 ppm to 0 ppm CO_2.

Fig. 5 shows the clear effect of vacuum level on the capacity profiles of the initial purge phase before any heating. At both vacuum levels, the working capacity is still rising after 30 min of purging, but especially with 25 mbar vacuum a steep rise can be seen for both TVSA and TVCSA processes. The 25 mbar vacuum purge capacity profiles are similar whether using air or nitrogen as purge gas, which can be explained by the very small CO_2 partial pressure difference of 0.01 mbar (10 ppmv) CO_2 in these vacuum conditions. With 500 mbar vacuum the purge-step desorption occurs very slowly for both processes. It was not assessed whether the isothermal purging alone could regenerate the adsorbent fully like it should be based on CO_2 isotherms [21], but it is clear this would take at least several hours, which would probably lead to a very energy-intensive process.

Fig. 5 shows that the first temperature swing to 60 °C leads to a rapid rise of working capacity in both TVSA and TVCSA processes. Comparing the temperature swing steps in TVSA to those of TSA, using even a mild vacuum of 500 mbar clearly enhances the desorption dynamics at 60 °C. For example, with 500 mbar vacuum in TVSA the working capacity gained during 30 min of heating is 0.44 $mmol_{CO2}/g_{sorbent}$, while for TSA this is 0.36 $mmol_{CO2}/g_{sorbent}$. Using a higher vacuum of 25 mbar leads to even faster desorption. For TVSA with 25 mbar vacuum, over 99% of the maximum capacity at 60 °C is reached within 20 min. However, using 500 mbar vacuum TVSA, this takes over 50 min and equilibrium is not reached after 1 h. The second temperature swing to 100 °C leads to a fast increase of working capacity like in the TSA process. For example, in the TVSA 500 mbar experiment reaching 99% of the maximum capacity at 100 °C takes less than 15 min from the start of 'TS 2'. With the higher vacuum level of 25 mbar the desorption at 100 °C is not significant anymore, which could also be seen from Fig. 3b.

In the closed TVSA runs, initial vacuum purge state produced only negligible amounts of capacity. This is further evidence to proving that isothermal vacuum swing adsorption without compression is not reasonable in DAC [21,23]. Therefore, Fig. 6 shows no observable increase in working capacity in this initial purge phase. However, the temperature swings quickly increase the working capacity with less than 1 min delay, as now there are no delays caused by gas travel time and sensor response like in the other experiments as mentioned above. For TVSA with temperature ramping, it takes about 7 min to reach 0.13 $mmol_{CO2}/g_{sorbent}$ in the first temperature swing to 60 °C. A higher temperature increases both working capacity and desorption rate considerably. For TVSA without temperature ramping, the increase from zero to 0.39 $mmol_{CO2}/g_{sorbent}$ takes about 5 min. The final working capacity in the temperature ramping case is about 0.04 $mmol_{CO2}/g_{sorbent}$ lower than in the experiment without temperature ramp. In addition to experimental uncertainty, the difference may be caused by

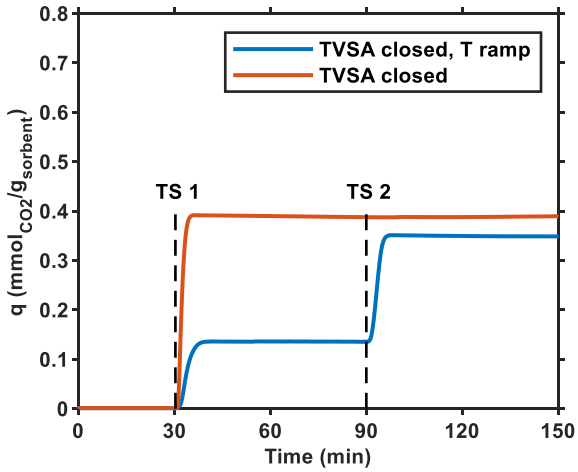

Fig. 6. Desorption capacity profiles in TVSA runs closed from inlet with and without temperature ramping. The initial period is vacuuming at 25 °C. With temperature ramping the temperature of the adsorbent was set to 60 °C after 'TS 1' and to 100 °C after 'TS 2'. Without temperature ramping the temperature was set to 100 °C directly after 'TS 1'.

very slowly continuing desorption of CO_2 after the initial period at 60 °C, in which case the flow rate is under the detection limit of the flow meter.

From the working capacity profiles the promoting effect of high vacuum and temperature on both final working capacities as well as dynamics is clear. Fairly good results were gained with the combination of mild vacuum and temperature as well. In the next chapter, specific energy requirements of TSA and TVSA with 40 ml/min air flow and closed TVSA processes are compared. TVCSA is omitted in the following discussion due to the results being fairly similar with TVSA.

3.3. Specific energy requirements of regeneration

Like explained in chapter 2.4, the following specific energy requirements (SER) are cumulative, taking into account the changes in experimental temperature, vacuum level, CO_2 capacity and gas flow. Because the energy requirement is divided by the capacity obtained until given time point, SER figures start from very high values because the first capacity values are close to zero. Only the contribution of the regeneration phase is taken into account in the following SER numbers because the adsorption phase was similar for all runs. Also, the flow rate during adsorption was 1000 ml/min, resulting in too high flow rate per mass of adsorbent ratio considering process scale. Also, it should be

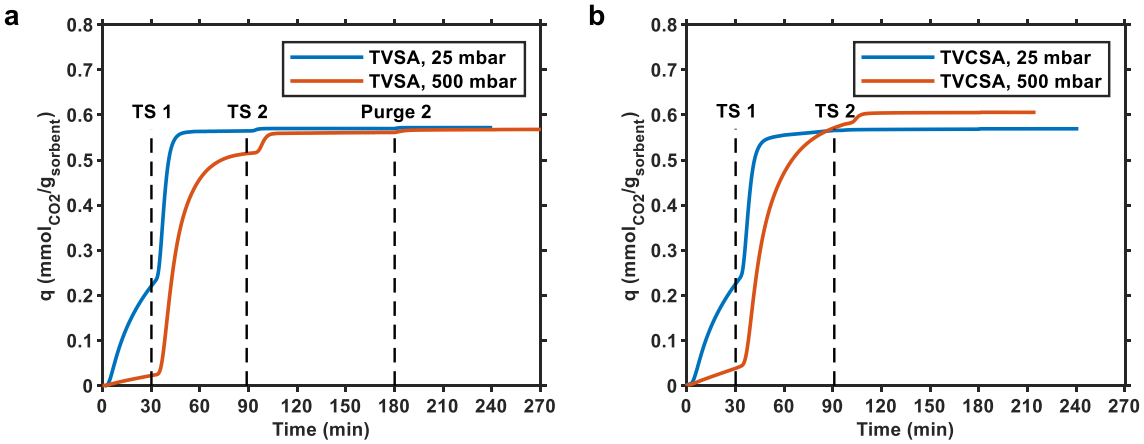

Fig. 5. Desorption capacity profiles under vacuum using 40 ml/min flow of a) 400 ppm CO_2; b) 0 ppm CO_2. The initial period is vacuuming at 25 °C. Temperature of the adsorbent was set to 60 °C after 'TS 1' and to 100 °C after 'TS 2'. 'Purge 2' refers to switching flow to pure N_2.

noted that most of the energy requirement in this analysis resulted from latent heat of adsorbent and vacuum energy. The contribution of fan energy was typically negligible due to short desorption time and low pressure drop over the adsorbent bed of typically below 30 Pa even though the bed height-to-diameter ratio was 4. Therefore, the results of this chapter only apply if the pressure drop is manageable, e.g. below 450 Pa such as in Bajamundi et al. [13], in a tall adsorption column.

The empty volume measured by the flow meter in an evacuation step was 80 ml. The energy consumed in evacuating the empty volume of the system has been subtracted from the total energy requirement in steps where vacuum was used. The reasoning for this is that in a practical process the amount of empty volume in the system would be minimized to reduce capital costs. Also, in a practical process the energy consumed by the evacuation step is only around a few percent of the total energy requirement [49], and therefore shouldn't affect the conclusions of the following specific energy requirement analysis. Working capacity is presented alongside the specific energy values, because working capacity is the meter for estimating daily production of CO_2. Also, working capacity is linked with the produced CO_2 purity in that with a constant flow rate the more produced working capacity within certain time, the higher the average purity is. With 40 ml/min inflow, the purities peaked to 1.3%, 1.8% and 2.7% during the first temperature swing for TSA, TVSA at 500 mbar and TVSA at 25 mbar, respectively. However, the produced CO_2 purities of the current small-scale column do not represent the actual purities in process scale due to high amount of empty volume (see Supplementary data Table S2), and therefore the purities are not shown as a function of time in the following analysis.

Fig. 7 shows that the specific energy requirement for the TSA process reaches the minimum of 4.2 MJ/kg_{CO2} at the end of the first temperature swing, at which point around 0.47 $mmol_{CO2}/g_{sorbent}$ has already been reached. After the second temperature swing the SER settles to 6.4 MJ/kg_{CO2}, with working capacity of 0.55 $mmol_{CO2}/g_{sorbent}$. Therefore, 17% increase in working capacity (0.08 $mmol_{CO2}/g_{sorbent}$) requires about 52% SER increase mainly caused by 40 °C higher desorption temperature. The actual additional SER increase may be even more due to increased cooling demand.

Fig. 8 shows that the SER in TVSA with 25 mbar vacuum rises very sharply with time. After the initial vacuum purge step, rapidly produced CO_2 reduces the SER, reaching the minimum of 26 MJ/kg_{CO2} at around 43 min. At this point the working capacity is about 0.53 $mmol_{CO2}/g_{sorbent}$ and still increasing. The working capacity of 0.56 $mmol_{CO2}/g_{sorbent}$ is reached at 50 min, at which point the SER is already 28 MJ/kg_{CO2}. After this point the working capacity increases only marginally, but the SER increases significantly. The high specific energy requirement in this case is caused by coupling relatively high vacuum with the fairly high regeneration flow rate to adsorbent mass ratio of 40 l/(min·kg). This ratio e.g. for the DAC demonstration unit reported earlier [13] is around 100 l/(min·kg) during adsorption. The DAC unit total SER was between 44 and 52 MJ/kg_{CO2} [13], of which the contribution of total regeneration energy has been determined to be around 60–70%. Therefore, the optimal SER values gained in this work with TVSA using 25 mbar vacuum and inlet flow of 40 ml/min are already near the SER of the demonstration unit that is by no means an optimal DAC process. This strongly imparts that the high-vacuum TVSA with purge flow is an unreasonable option for process scale regeneration.

Lowering the vacuum level reduces the SER significantly for TVSA with inlet flow. Although not shown in Fig. 9, after the initial vacuum purge step the SER first increases higher than in TVSA with 25 mbar vacuum, which is caused by slower desorption of CO_2. However, the SER then decreases to the minimum of 6.9 MJ/kg_{CO2} at 63 min, at which point the reached working capacity is 0.47 $mmol_{CO2}/g_{sorbent}$. For comparison, to reach the same working capacity in the TSA required 39% smaller SER. Continuing the desorption until 90 min increases the working capacity to 0.51 $mmol_{CO2}/g_{sorbent}$ and comes with the SER of 7.5 MJ/kg_{CO2}. The increase in both SER and working capacity is around 9%. Therefore, in this case stopping the desorption process at SER minimum cannot be recommended. Although the SER values are significantly lower with the milder vacuum, the process is slowed down. For example, reaching the SER minimum after the start of heating took only 13 min in the 25 mbar process, while for the 500 mbar process this took 33 min. Temperature swing to 100 °C for the 500 mbar TVSA increases the working capacity to 0.56 $mmol_{CO2}/g_{sorbent}$ and the SER to over 10 MJ/kg_{CO2}, corresponding to approximately 10% and 33% increases in SER and working capacity, respectively.

Fig. 10 shows that after the initial vacuum purge and first temperature swing, the SER of closed TVSA settles to 11 MJ/kg_{CO2} with working capacity of 0.14 $mmol_{CO2}/g_{sorbent}$. After the second temperature swing the SER settles to 9.4 MJ/kg_{CO2} with a working capacity of 0.35 $mmol_{CO2}/g_{sorbent}$. However, in another experiment where the temperature was directly ramped to 100 °C the maximum working capacity was 0.39 $mmol_{CO2}/g_{sorbent}$, with a lower SER value of 8.6 MJ/kg_{CO2}. Therefore, for closed TVSA using a higher regeneration temperature is not only highly recommended in terms of working capacity, but also beneficial in terms of the specific energy requirement.

Table 2 summarizes the results of working capacity and SER for the different regeneration methods. The results are from a time point after which the desorption rate slows down significantly. With 60 °C and 100 °C temperature swing this point marked reaching 90% and 99% of the maximum working capacity of the step, respectively. With 60 °C temperature swing this point was also at or near the minimum SER value. Also, daily productivities were calculated using these working capacities and the amount of cycles per day. The amount of cycles per day was calculated using a cycle structure with desorption times in Table 2 and fixed adsorption and cooling times of 120 min and 30 min, respectively. In Table 2, TCSA rather than TSA values should be used for comparison of productivities because it has the same initial purge step than other regeneration options. It should also be stressed that comparing the 60 °C productivity values directly with the 100 °C values is not fair in most cases due to temperature ramping in all except 'TVSA closed'. With 60 °C desorption temperature, TCSA has a lower productivity of 0.122 $kg_{CO2}/(kg_{adsorbent}·d)$ compared to 0.139 and 0.150 $kg_{CO2}/(kg_{adsorbent}·d)$ for TVSA and TVCSA with mild vacuum, respectively. Because closed TVSA has the lowest working capacities with both desorption temperatures, the productivities are also lower compared to other options, except when using direct heating to 100 °C. Closed TVSA also has higher SER values compared to TSA/TCSA or the mild vacuum TVSA/TVCSA at 60 °C, even with direct heating to 100 °C. On the other hand, the SER values of mild vacuum TVSA/TVCSA are higher than for TSA/TCSA.

Few examples can be found in the literature where purge flow with vacuum is assessed as a regeneration method for amine-based adsorbent CO_2 capture. Serna-Guerrero et al. [50] found increased desorption

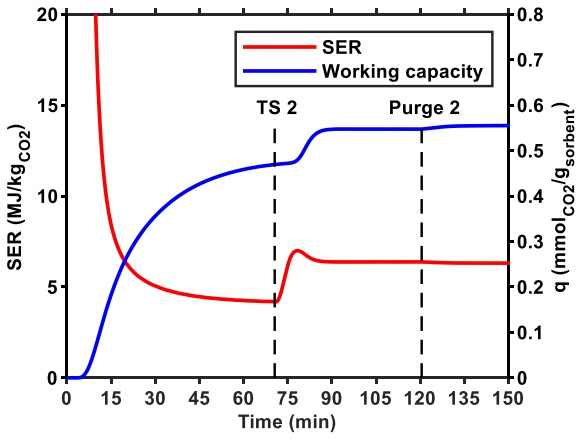

Fig. 7. Dynamic specific energy requirement (SER) and working capacity profiles for temperature-swing adsorption with 40 ml/min total flow rate of 400 ppm CO_2.

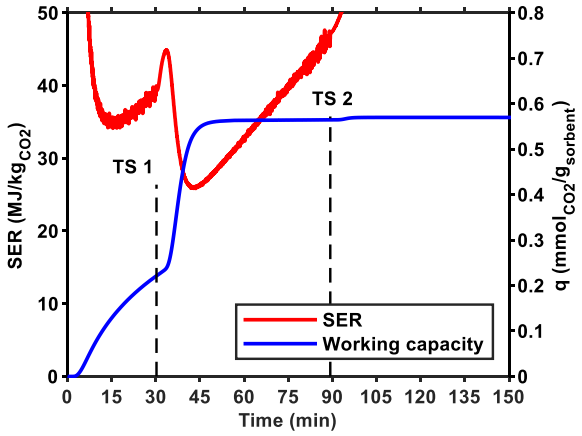

Fig. 8. Dynamic specific energy requirement (SER) and working capacity profiles for temperature-vacuum swing adsorption with 40 ml/min total flow rate of 400 ppm CO_2 and 25 mbar vacuum.

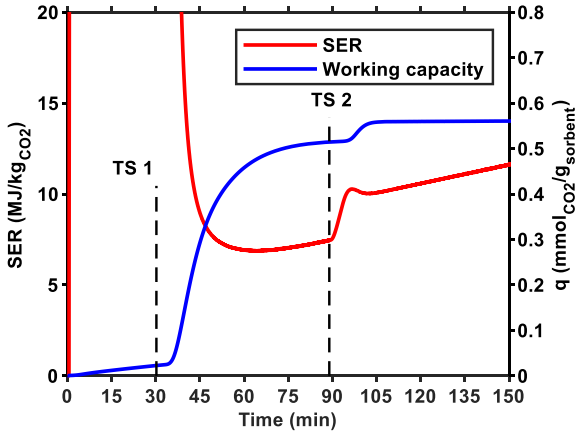

Fig. 9. Dynamic specific energy requirement (SER) and working capacity profiles for temperature-vacuum swing adsorption with 40 ml/min total flow rate of 400 ppm CO_2 and 500 mbar vacuum.

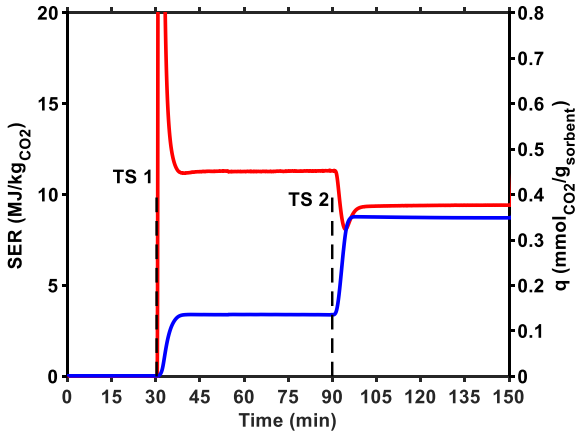

Fig. 10. Dynamic specific energy requirement (SER) and working capacity profiles for temperature-vacuum swing adsorption at 11 mbar vacuum.

rates with an amine-grafted mesoporous silica adsorbent when using purge gas coupled with TVS desorption. On the other hand, Wijesiri et al. [30] found lower desorption rates for the TVS desorption with N_2 purge compared to using steam as purge with a polyethylenimine-functionalized mesoporous silica adsorbent. However, these studies did not assess the total specific energy requirement of the process. Bos et al. [19] compared the regeneration options for biogas upgrading using a commercial amine-functionalized polystyrene resin, and also considered TVSA case with 100 mbar vacuum and 60 °C with air purge. This option had otherwise low regeneration energy requirement compared to other options, but the contribution of vacuum was almost equal to the heat demand, therefore leading to the highest total energy requirement of the considered cases. Like in this work, Bos et al. found that if only considering SER, TSA/TCSA was the most attractive option.

In a later work, Bos et al. [18] compared regeneration options for DAC, but didn't consider the option with vacuum combined with air or inert gas as purge flow. In dry conditions, they reported much higher SER values for PTSA (closed TVSA) than in this work, even though the reported working capacities of less than 0.25 mmol$_{CO2}$/g$_{sorbent}$ at 91 °C are not very far from those in this work. However, at a higher temperature of 116 °C the SER in Bos et al. was around 10 MJ/kg$_{CO2}$, which is close to the values in this work. As an interesting result, the specific energy requirement decreased with co-adsorbed water, but increased if steam-stripping was applied. Wurzbacher et al. [31] reported working capacities of 0.32–0.65 mmol$_{CO2}$/g$_{sorbent}$ for (closed) TVSA process in humid conditions in adsorption. They also reported the SER values of 493–640 kJ/mol$_{CO2}$ (11.2–14.5 MJ/kg$_{CO2}$), with increase as a function of humidity content in air. Although the boosting effect of humidity on working capacity has been shown also for the sorbent in this work [21], the effect of humidity on SER during regeneration is not obvious, and should be assessed in future work in detail.

Based on the results of chapters 3.2 and 3.3, a mild vacuum TVSA with purge flow doesn't have unreasonably high energy requirement, as long as the purge flow rate is not unreasonably high. Also, even 40 ml/min is high for the sample size of 1 g considering a practical process, and it is possible that significantly lower specific energy requirements are obtainable for TVSA with purging flow when the flow rate and sample size are properly scaled. On the other hand, the boost in productivity from using purge flow during vacuum may still be worth a higher energy requirement. However, it should be taken into account that the differences in productivity between TSA/TCSA vs. TVSA/TVCSA may be smaller in cases where adsorption phase is much longer than desorption, as the effect of desorption rate becomes less significant. On the other hand, the contrary is true for closed TVSA compared to other methods, because less working capacity per cycle means lower daily productivity when the amount of cycles per day is smaller. The results therefore confirm the equilibrium modelling result [21] that the use of closed TVSA process for other utilization purposes than those that require 100% CO_2 cannot be recommended in terms of productivity. Also, because of the lower working capacity, the closed TVSA process has a higher specific energy requirement than the methods utilizing inlet purge flow with or without mild vacuum. However, before assessing adsorbent regenerability, no conclusions of the overall performance of each regeneration method can be made.

3.4. Cyclic experiments

All cyclic experiments done with 19–23 cycles lead to a capacity decrease, which means that the aminoresin studied here started to lose capacity even with a relatively low number of cycles. Significant capacity drops for amine-based adsorbents in only a few cycles have in some cases been measured, while in some cases the sorbent has lasted 100 cycles or more with less than 10% capacity decrease [25]. For example, for the commercial amine-based sorbent Lewatit VP OC 1065, no capacity decrease was noted in 50–60 cycles in various desorption conditions [18,19], and only 4.8% loss of capacity was found in 275 cycles with desorption in N_2 flow at 105 °C [51]. However, in this work, significant differences in adsorbent regenerability were found between the studied regeneration methods.

Fig. 11 shows the slightly decreasing trend of cyclic adsorption and desorption capacity over 19 TCSA cycles. Fig. 11b shows that in adsorption capacities there is a significant drop of about 0.03 mmol/g when comparing the first and third cycles. After this, the adsorption

Table 2
Working capacities, productivities and specific energy requirements at 90% and 99% of maximum working capacity at desorption temperatures of 60 °C and 100 °C, respectively. Total flow rate during desorption was 40 ml/min in other experiments except TVSA closed and TVSA closed with temperature ramp. All other experiments were done using temperature ramping to 60 °C and then 100 °C except TVSA closed. Uncertainties based on uncertainty of capacity.

Regeneration method	WC ($mmol_{CO2}/g_{adsorbent}$)		Time (min)		Productivity ($kg_{CO2}/(kg_{adsorbent}·d)$		Regeneration SER (MJ/kg_{CO2})	
	90%, 60 °C	99%, 100 °C	90%, 60 °C	99%, 100 °C	90%, 60 °C	99%, 100 °C	90%, 60 °C	99%, 100 °C
TSA	0.423 ± 0.014	0.542 ± 0.018	43.9	85.9	0.138 ± 0.005	0.146 ± 0.005	4.5 ± 0.2	6.4 ± 0.2
TCSA	0.434 ± 0.015	0.551 ± 0.019	74.9	117.8	0.122 ± 0.004	0.130 ± 0.004	4.4 ± 0.1	6.3 ± 0.2
TVSA, 25 mbar	0.508 ± 0.017	0.564 ± 0.019*	41.2	72.4	0.168 ± 0.006	0.161 ± 0.005	26.2 ± 0.9	38.4 ± 1.3
TVSA, 500 mbar	0.463 ± 0.016	0.555 ± 0.019	61	102.4	0.139 ± 0.005	0.139 ± 0.005	6.9 ± 0.2	10.0 ± 0.3
TVCSA, 25 mbar	0.509 ± 0.017	0.563 ± 0.019*	42.4	82.5	0.168 ± 0.006	0.153 ± 0.005	26.1 ± 0.9	41.7 ± 1.4
TVCSA, 500 mbar	0.515 ± 0.018	0.599 ± 0.02	68.1	106.7	0.150 ± 0.005	0.148 ± 0.005	6.2 ± 0.2	9.0 ± 0.3
TVSA closed, T ramp	0.122 ± 0.005	0.345 ± 0.014	36.3	95.7	0.042 ± 0.002	0.089 ± 0.004	11.7 ± 0.5	8.5 ± 0.3
TVSA closed	–	0.386 ± 0.016	–	34.6	–	0.133 ± 0.005	–	7.5 ± 0.3

* Working capacity was already achieved at 60 °C.

capacities show no significant drop for at least the next 6 cycles. The desorption capacities show a fairly steadily decreasing trend rather than a significant drop in the first few cycles. Overall, the drop in capacity over 19 cycles is approximately from 0.57 to 0.53 $mmol_{CO2}/g_{adsorbent}$ (7%) and from 0.53 to 0.51 $mmol_{CO2}/g_{adsorbent}$ (4%) in adsorption and desorption, respectively. The significant drop at the start for the adsorption capacities may be related to incomplete regeneration during the cyclic desorption phases, the effect of which mostly disappears after a couple of cycles, leading to stabilization of the cyclic adsorption capacity. Therefore, the decrease in desorption capacities may be the more reliable metric for long-term regenerability in the TCSA case.

To gain an idea of how high decrease of capacity in cyclic conditions can be expected in the worst case, cyclic test was done using TVS regeneration mechanism at 200 mbar vacuum, 100 °C and 1000 ml/min flow of compressed dry air. Fig. 12 shows that the decrease of adsorption and desorption capacities in the TVSA cycles is significant due to coupling high temperature with oxygen-containing gas. Fig. 12a shows an increase in the purge capacities before temperature swing like in the TCSA cycles in Fig. 11, which may be related to positive sensor drift (see Supplementary data). However, both the adsorption and total desorption capacities decrease from approximately 0.52 to 0.45 $mmol_{CO2}/g_{adsorbent}$ (13%) over 22 cycles. It is also notable from these numbers and from Fig. 12b that this time the adsorption and desorption capacities are very close to each other, the maximum difference being within 0.01 $mmol_{CO2}/g_{adsorbent}$. The main reason for this probably lies in almost complete regeneration due to coupled vacuum and concentration swing with a high flow rate. Also, the method of capacity calculation was changed after the cyclic TCSA run so that instead of measuring the step function (see chapter 2.3) only at the start of the cyclic experiment, it was measured at the start of each cycle. This method may yield more accurate results and was thus used in the processing of consequent cyclic experiment results.

The same regeneration method was then used for cyclic runs but this time with temperature swing to only 60 °C. Fig. 13 shows that the decrease of both adsorption and total desorption capacities is now only from approximately 0.53 to 0.50 $mmol_{CO2}/g_{adsorbent}$ (6%) in 22–23 cycles. The last three cycles do not show a decreasing trend in capacity, although from this number of cycles it is still too early to draw any conclusions whether the decrease has stabilized or not. Compared to the 100 °C case, the cyclic working capacities with 60 °C temperature swing are slightly smaller, although only less than 10%.

Fig. 14 shows that in the cyclic closed TVSA runs only mild decrease of adsorption capacity took place. It should be noted, that after the closed TVS desorption step the column was purged with nitrogen to fully regenerate the sorbent between each cycle. The desorption capacities shown in Fig. 14a are only the contribution of closed TVS desorption. The adsorption and desorption capacities decrease from approximately 0.53 to 0.49 $mmol_{CO2}/g_{adsorbent}$ (8%) and 0.37 to 0.31 $mmol_{CO2}/g_{adsorbent}$ (16%), respectively. In the desorption capacities most of the decrease takes place between the first two cycles, in which it drops from 0.37 to 0.33 $mmol_{CO2}/g_{adsorbent}$. If not taking into account this initial drop, the capacity decrease from the second to 23rd cycle is only 0.02 $mmol_{CO2}/g_{adsorbent}$ (6%), being close to the capacity decrease in the adsorption results.

Calculating the desorption capacity loss in percent per cycle, the precise values are 0.18, 0.26, and 0.60%/cycle for TCSA, TVSA with air flow at 60 °C and 100 °C, respectively. For TVSA closed the capacity decrease from adsorption results is 0.38%/cycle. Although the

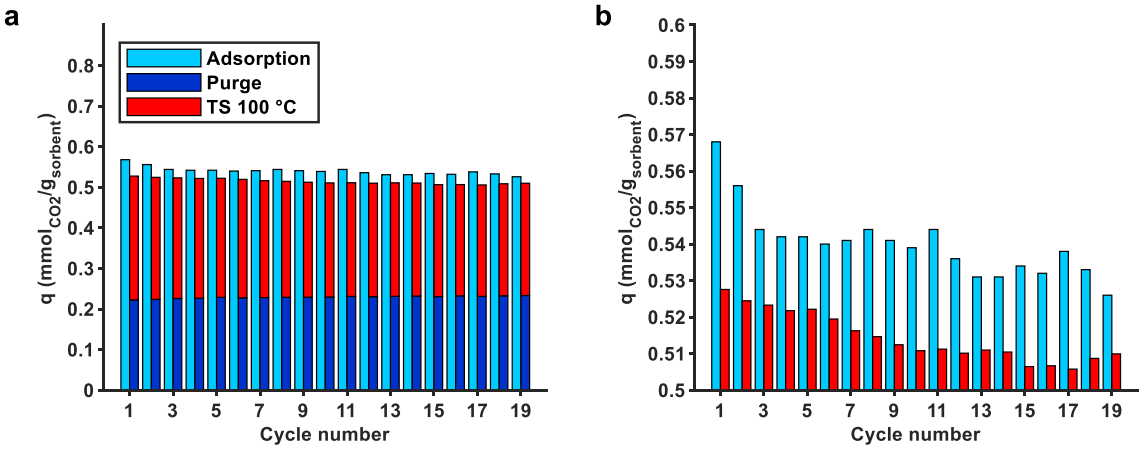

Fig. 11. CO_2 adsorption and desorption capacities in repeated cycles of temperature-concentration swing adsorption. Adsorption was done using 400 ppm CO_2/N_2. b) is a close-up of a).

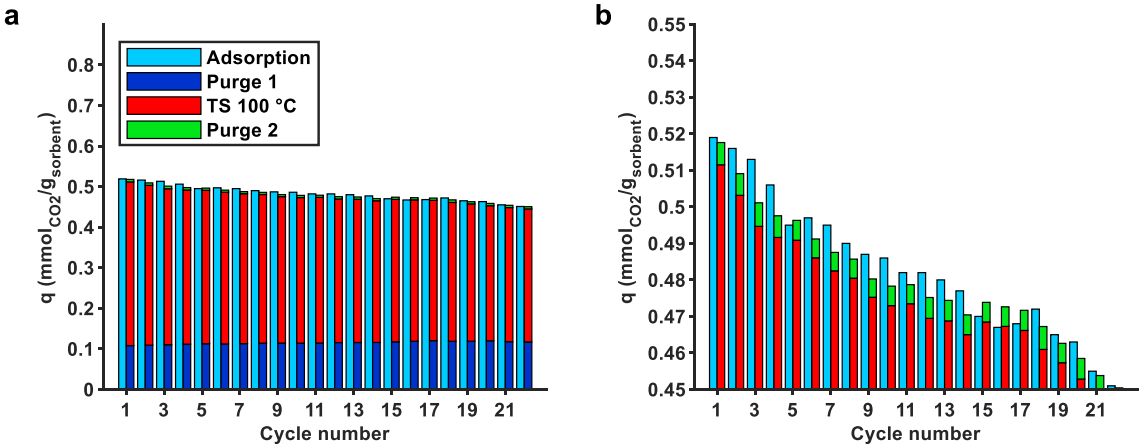

Fig. 12. CO_2 adsorption and desorption capacities in repeated cycles of temperature-vacuum swing adsorption with also concentration swing ('Purge 2') at the end. Adsorption and desorption before 'Purge 2' were done using compressed air. b) is a close-up of a).

desorption in the TCSA process was conducted in inert conditions, the slight capacity decrease is in line with literature, as capacity decrease using inert purge such as N_2 at elevated temperatures has been noted for both impregnated and grafted amine adsorbents [25]. The second-lowest capacity decrease for the 60 °C TVSA with air purge can perhaps be explained with slight oxidative degradation, although for example Bos et al. [19] found that oxidative degradation in a 1 h test did not begin until the temperature was at 70 °C for the commercial Lewatit VP OC 1065. The largest capacity decrease for TVSA with air flow at 100 °C imparts significant oxidative degradation taking place. This is because the capacity loss is much higher than in the 100 °C TCSA cycles, which are devoid of air during desorption.

In the case of the closed TVSA process, no oxygen should be present during desorption due to evacuation of the adsorption column, but the cyclic capacity loss is still higher than in TVSA with air flow at 60 °C. The stability of an amine-functionalized nanofibrillated cellulose sorbent was studied in 100 cycles of closed TVSA cycles by Gebald et al. [35], who reported only 5% of capacity decrease, although at a lower temperature of 90 °C. They also reported that in TVS operation the degradation was attributed to loss of amines and formation of amides or imides. However, it was unclear whether both were the cause of residual oxygen in the system, or that loss of amines could occur by thermal degradation only. In any case, it seems that degradation of amine-functionalized sorbents cannot be avoided with the closed TVSA method, since lowering the desorption temperature is not a reasonable option due to lowered working capacities.

Based on the working capacity and specific energy requirement results of this study, regeneration options that utilize purge flow are more flexible in terms of regeneration temperature than the closed TVSA method. To avoid the loss of capacity, the regeneration temperature should be maintained well below 100 °C. In this regard, the mild vacuum TVSA process coupled with purge flow and low temperature seems promising in terms of all studied aspects: working capacity, specific energy requirement and adsorbent regenerability. However, even in mild desorption conditions the cyclic capacity drops per cycle predict only a few hundred cycles before all of the capacity is lost, while in practice the sorbent should withstand thousands if not tens of thousands of cycles with realistic adsorbent costs [22]. On the other hand, it is not known whether the capacity drop follows a linear trend, stabilizes at some point or even accelerates. Also, in inert conditions or in vacuum, the actual mechanism for degradation is less obvious than in the presence of air, and it is not known if for example the vacuum level has an effect on the loss of capacity along with temperature. Therefore, further work is required in cyclic process comparison that takes into account these aspects as well.

4. Conclusions

In this study, a detailed experimental comparison of regeneration methods for CO_2 capture from air was made using an amine-functionalized adsorbent. The experiments were conducted with an automated fixed-bed CO_2 adsorption and desorption device. Especially, the focus was in comparing methods that produce low-purity CO_2 with closed inlet TVSA that produces pure CO_2. The working capacity, dynamics of

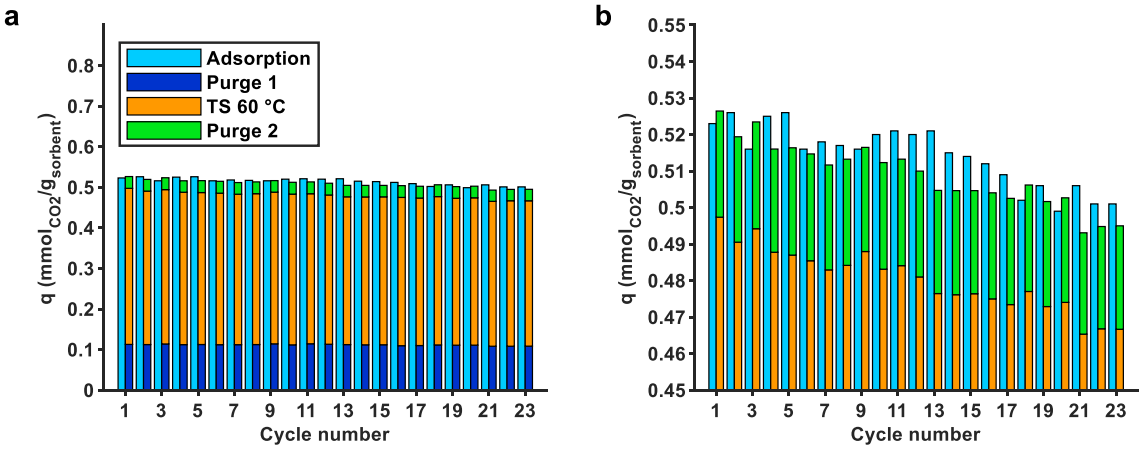

Fig. 13. CO_2 adsorption and desorption capacities in repeated cycles of temperature-vacuum swing adsorption with also concentration swing ('Purge 2′) at the end. Adsorption and desorption before 'Purge 2′ were done using compressed air. b) is a close-up of a).

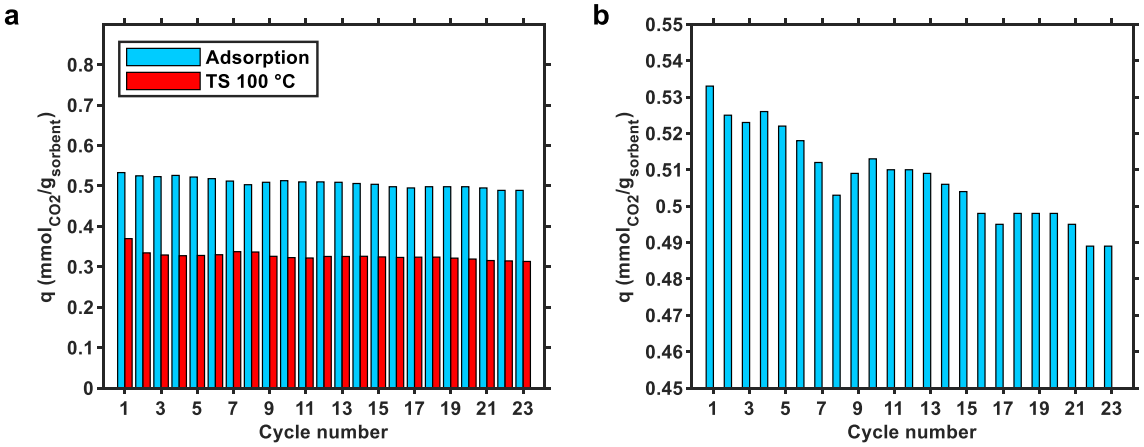

Fig. 14. CO_2 adsorption and desorption capacities in repeated cycles of temperature-vacuum swing adsorption with closed inlet. Adsorption was done using compressed air. After 'TS 100 °C' the sample was fully regenerated by maintaining temperature at 100 °C and purging with nitrogen under vacuum. b) is a close-up of a).

desorption and specific energy requirement were evaluated for TSA, TCSA and TVSA with or without purge flow. Also, regenerability in TCSA and TVSA processes with and without purge flow was studied over 19–23 adsorption and desorption cycles. Coupling vacuum and temperature swing with inlet flow has not been assessed as a regeneration method for DAC in detail before.

Working capacity comparison showed that TSA/TCSA at 60 °C is sufficient to reach 85–86% regeneration, while coupling purge flow with vacuum in TVSA/TVCSA leads to over 90% regeneration. However, using closed TVSA process with no inlet flow left the adsorbent with significant residual loading even at 100 °C. The lowest minimum regeneration specific energy requirement of 4.2 MJ/kg$_{CO2}$ was achieved with isobaric TSA at 60 °C with the working capacity of 0.47 mmol$_{CO2}$/g$_{sorbent}$. TVSA at 25 mbar with air flow gave high regeneration SER of over 26 MJ/kg$_{CO2}$. However, utilizing a mild vacuum of 500 mbar lead to only 7.5 MJ/kg$_{CO2}$ with working capacity of 0.51 mmol$_{CO2}$/g$_{sorbent}$. The TVSA process with no inlet flow had the regeneration SER of 8.6 MJ/kg$_{CO2}$ with the maximum achievable capacity of only 0.39 mmol$_{CO2}$/g$_{sorbent}$.

Determination of dynamic working capacity allowed the calculation of daily productivities, which with 60 °C regeneration temperature were 0.122 and 0.150 kg$_{CO2}$/(kg$_{adsorbent}$·d) for TCSA and 500 mbar TVCSA with purge flow, respectively. TVSA with air flow at 500 mbar had a slightly lower productivity than TVCSA of 0.139 kg$_{CO2}$/(kg$_{adsorbent}$·d). The productivity for TVSA with no inlet flow was 0.133 kg$_{CO2}$/(kg$_{adsorbent}$·d) at 100 °C, being lower than for the regeneration options utilizing vacuum coupled with purge flow. In cyclic adsorption/desorption tests the current adsorbent showed a significant capacity loss of 0.6% per cycle at 100 °C with vacuum and air flow. Even with air evacuated out, a capacity loss of 0.38% per cycle was found for the closed inlet TVSA process. Lowering the desorption temperature to 60 °C was highly beneficial for the TVSA method with air flow, because the capacity loss was then only 0.26% per cycle, while still over 90% regeneration was maintained.

The results of this study impart that TVSA coupled with air or inert gas purge flow has clear productivity benefits compared to either isobaric TSA/TCSA or the closed inlet TVSA process. While coupling high vacuum with purge flow leads to unreasonably high energy consumption, mild vacuum can be used to keep the SER lower than in the TVSA process with no inlet flow. The lowest possible specific energy requirements can be obtained using isobaric TSA/TCSA. Flow from the inlet side allows a low regeneration temperature of 60 °C, which cannot be achieved with the closed TVSA process due to drastically reduced working capacity. Even though the column is evacuated of air in the closed TVSA process, degradation of the adsorbent cannot be avoided if even moderate working capacity has to be achieved. Consequently, mild vacuum TVSA with air flow at 60 °C leads to a better regenerability of the adsorbent. Overall, mild vacuum and temperature TVSA/TVCSA coupled with purge flow seems a viable option for low-concentration CO_2 production from air. The low regeneration temperature also allows the use of process waste heat or district heating in this process or in TSA/TCSA. Therefore, in applications such as greenhouses or microbial and algae cultivation, TSA, TCSA or these coupled with mild vacuum should be the preferred options to the closed TVSA process.

The current study is however limited only to dry conditions with reasonable boundaries for temperature and an upper limit for the flow-rate. In future studies, productivity and specific energy requirement should be assessed as a function of temperature and flow-rate, which could be achieved e.g. by combining experimental work with dynamic modelling. Also, the process scale limitations related to heat transfer, vacuum pumps and purge gas cost should be taken into account. The effect of humidity on process dynamics and specific energy requirement also needs to be evaluated. Adsorbent regenerability should also be studied with a wider set of conditions and even more cycles. Particularly, the different modes of TSA and TVSA should be compared with the steam-stripping method in terms of specific energy requirement and adsorbent regenerability. Also, it should be confirmed whether long-term exposure to desorption conditions or repeated shift between adsorption and desorption conditions is the main driver for degradation. This information would help in deciding whether to maximize daily productivity by maximizing capacity per cycle or by minimizing the cycle duration.

Declaration of Competing Interest

The authors declare that they have no known competing financial interests or personal relationships that could have appeared to influence the work reported in this paper.

Acknowledgements

This study was conducted as a part of projects funded by Academy of Finland under grant numbers 295883 and 329312.

Appendix A. Supplementary data

Supplementary data to this article can be found online at https://doi.org/10.1016/j.cej.2020.126337.

References

[1] Y. Wang, L. Zhao, A. Otto, M. Robinius, D. Stolten, A review of post-combustion CO_2 capture technologies from coal-fired power plants, Energy Proc. 114 (2017) 650–665, https://doi.org/10.1016/j.egypro.2017.03.1209.

[2] W. Zhang, H. Liu, Y. Sun, J. Cakstins, C. Sun, C.E. Snape, Parametric study on the regeneration heat requirement of an amine-based solid adsorbent process for post-combustion carbon capture, Appl. Energy 168 (2016) 394–405, https://doi.org/10.1016/j.apenergy.2016.01.049.

[3] X. Chen, G. Huang, C. An, Y. Yao, S. Zhao, Emerging N-nitrosamines and N-nitramines from amine-based post-combustion CO_2 capture – A review, Chem. Eng. J. 335 (2018) 921–935, https://doi.org/10.1016/j.cej.2017.11.032.

[4] Z. Zhang, Y. Li, W. Zhang, J. Wang, M.R. Soltanian, A.G. Olabi, Effectiveness of amino acid salt solutions in capturing CO_2: A review, Renew. Sustain. Energy Rev. 98 (2018) 179–188, https://doi.org/10.1016/j.rser.2018.09.019.

[5] D.W. Keith, M. Ha-Duong, J.K. Stolaroff, Climate strategy with CO_2 capture from the air, Clim. Change 74 (2006) 17–45, https://doi.org/10.1007/s10584-005-9026-x.

[6] R. Socolow, M. Desmond, R. Aines, J. Blackstock, O. Bolland, T. Kaarsberg, N. Lewis, M. Mazzotti, A. Pfeffer, K. Sawyer, J. Siirola, B. Smit, J. Wilcox, Direct air capture of CO_2 with chemicals – A technology assessment for the APS Panel on Public Affairs, APS Phys. (2011).

[7] D.W. Keith, G. Holmes, D. St, K.H. Angelo, A process for capturing CO_2 from the atmosphere, Joule 2 (2018) 1573–1594, https://doi.org/10.1016/j.joule.2018.05.006.

[8] S. Choi, J.H. Drese, C.W. Jones, Adsorbent materials for carbon dioxide capture from large anthropogenic point sources, ChemSusChem 2 (2009) 796–854, https://doi.org/10.1002/cssc.200900036.

[9] S.Y. Lee, S.J. Park, A review on solid adsorbents for carbon dioxide capture, J. Ind. Eng. Chem. 23 (2015) 1–11, https://doi.org/10.1016/j.jiec.2014.09.001.

[10] A.E. Creamer, B. Gao, Carbon-based adsorbents for postcombustion CO_2 capture: A critical review, Environ. Sci. Technol. 50 (2016) 7276–7289, https://doi.org/10.1021/acs.est.6b00627.

[11] E.S. Sanz-Pérez, C.R. Murdock, S.A. Didas, C.W. Jones, Direct capture of CO_2 from ambient air, Chem. Rev. 116 (2016) 11840–11876, https://doi.org/10.1021/acs.chemrev.6b00173.

[12] Climeworks CO2 capture plant, (2020). https://www.climeworks.com/our-products/ (accessed February 21, 2020).

[13] C.J.E. Bajamundi, J. Koponen, V. Ruuskanen, J. Elfving, A. Kosonen, J. Kauppinen, J. Ahola, C.J.E. Bajamundi, J. Koponen, V. Ruuskanen, J. Elfving, A. Kosonen, J. Kauppinen, J. Ahola, Capturing CO_2 from air: Technical performance and process control improvement, J. CO2 Util. 30 (2019) 232–239, https://doi.org/10.1016/j.jcou.2019.02.002.

[14] K. Sumida, D.L. Rogow, J.A. Mason, T.M. McDonald, E.D. Bloch, Z.R. Herm, T.H. Bae, J.R. Long, Carbon dioxide capture in metal-organic frameworks, Chem. Rev. 112 (2012) 724–781, https://doi.org/10.1021/cr2003272.

[15] X. Shi, H. Xiao, H. Azarabadi, J. Song, X. Wu, X. Chen, K.S. Lackner, Sorbents for the direct capture of CO_2 from ambient air, Angew. Chem. Int. Ed. 59 (2020) 6984–7006, https://doi.org/10.1002/anie.201906756.

[16] G. Qi, L. Fu, E.P. Giannelis, Sponges with covalently tethered amines for high-efficiency carbon capture, Nat. Commun. 5 (2014) 1–7, https://doi.org/10.1038/ncomms6796.

[17] P.Q. Liao, X.W. Chen, S.Y. Liu, X.Y. Li, Y.T. Xu, M. Tang, Z. Rui, H. Ji, J.P. Zhang, X.M. Chen, Putting an ultrahigh concentration of amine groups into a metal-organic framework for CO_2 capture at low pressures, Chem. Sci. 7 (2016) 6528–6533, https://doi.org/10.1039/c6sc00836d.

[18] M.J. Bos, S. Pietersen, D.W.F.F. Brilman, Production of high purity CO_2 from air using solid amine sorbents, Chem. Eng. Sci. X. 2 (2019) 100020, , https://doi.org/10.1016/j.cesx.2019.100020.

[19] M.J. Bos, V. Kroeze, S. Sutanto, D.W.F. Brilman, Evaluating regeneration options of solid amine sorbent for CO_2, Ind. Eng. Chem. Res. 57 (2018) 11141–11153, https://doi.org/10.1021/acs.iecr.8b00768.

[20] W.R. Lee, S.Y. Hwang, D.W. Ryu, K.S. Lim, S.S. Han, D. Moon, J. Choi, C.S. Hong, Diamine-functionalized metal–organic framework: exceptionally high CO2 capacities from ambient air and flue gas, ultrafast CO_2 uptake rate, and adsorption mechanism, Energy Environ. Sci. 7 (2014) 744–751, https://doi.org/10.1039/c3ee42328j.

[21] J. Elfving, C. Bajamundi, J. Kauppinen, T. Sainio, Modelling of equilibrium working capacity of PSA, TSA and TVSA processes for CO_2 adsorption under direct air capture conditions, J. CO2 Util. 22 (2017) 270–277, https://doi.org/10.1016/j.jcou.2017.10.010.

[22] H. Azarabadi, K.S. Lackner, A sorbent-focused techno-economic analysis of direct air capture, Appl. Energy 250 (2019) 959–975, https://doi.org/10.1016/j.apenergy.2019.04.012.

[23] J.A. Wurzbacher, C. Gebald, A. Steinfeld, Separation of CO_2 from air by temperature-vacuum swing adsorption using diamine-functionalized silica gel, Energy Environ. Sci. 4 (2011) 3584–3592, https://doi.org/10.1039/c1ee01681d.

[24] A. Ahmadalinezhad, A. Sayari, Oxidative degradation of silica-supported polyethylenimine for CO_2 adsorption: insights into the nature of deactivated species, PCCP 16 (2014) 1529–1535, https://doi.org/10.1039/c3cp53928h.

[25] M. Jahandar Lashaki, S. Khiavi, A. Sayari, Stability of amine-functionalized CO_2 adsorbents: A multifaceted puzzle, Chem. Soc. Rev. 48 (2019) 3320–3405, https://doi.org/10.1039/c8cs00877a.

[26] W. Buijs, Direct air capture of CO_2 with an amine resin: a molecular modeling study of the deactivation mechanism by CO_2, Ind. Eng. Chem. Res. 58 (2019) 14705–14708, https://doi.org/10.1021/acs.iecr.9b02637.

[27] W. Li, S. Choi, J.H. Drese, M. Hornbostel, G. Krishnan, P.M. Eisenberger, C.W. Jones, Steam-stripping for regeneration of supported amine-based CO_2 adsorbents, ChemSusChem 3 (2010) 899–903, https://doi.org/10.1002/cssc.201000131.

[28] M.A. Sakwa-Novak, C.W. Jones, Steam induced structural changes of a poly(ethylenimine) impregnated γ-alumina sorbent for CO_2 extraction from ambient air, ACS Appl. Mater. Interfaces 6 (2014) 9245–9255, https://doi.org/10.1021/am501500q.

[29] W. Chaikittisilp, H.J. Kim, C.W. Jones, Mesoporous alumina-supported amines as potential steam-stable adsorbents for capturing CO_2 from simulated flue gas and ambient air, Energy Fuels 25 (2011) 5528–5537, https://doi.org/10.1021/ef201224v.

[30] R.P. Wijesiri, G.P. Knowles, H. Yeasmin, A.F.A. Hoadley, A.L. Chaffee, Desorption process for capturing CO_2 from air with supported amine sorbent, Ind. Eng. Chem. Res. 58 (2019) 15606–15618, https://doi.org/10.1021/acs.iecr.9b03140.

[31] J.A. Wurzbacher, C. Gebald, N. Piatkowski, A. Steinfeld, Concurrent separation of CO_2 and H_2O from air by a temperature-vacuum swing adsorption/desorption cycle, Environ. Sci. Technol. 46 (2012) 9191–9198.

[32] S. Choi, M.L. Gray, C.W. Jones, Amine-tethered solid adsorbents coupling high adsorption capacity and regenerability for CO_2 capture from ambient air, ChemSusChem 4 (2011) 628–635, https://doi.org/10.1002/cssc.201000355.

[33] L.A. Darunte, A.D. Oetomo, K.S. Walton, D.S. Sholl, C.W. Jones, Direct air capture of CO_2 using amine functionalized MIL-101(Cr), ACS Sustain. Chem. Eng. 4 (2016) 5761–5768, https://doi.org/10.1021/acssuschemeng.6b01692.

[34] A.R. Sujan, S.H. Pang, G. Zhu, C.W. Jones, R.P. Lively, Direct CO_2 capture from air using poly(ethylenimine)-loaded polymer/silica fiber sorbents, ACS Sustain. Chem. Eng. 7 (2019) 5264–5273, https://doi.org/10.1021/acssuschemeng.8b06203.

[35] C. Gebald, J.A. Wurzbacher, P. Tingaut, A. Steinfeld, Stability of amine-functionalized cellulose during temperature-vacuum-swing cycling for CO_2 capture from air, Environ. Sci. Technol. 47 (2013) 10063–10070, https://doi.org/10.1021/es401731p.

[36] Q. Yu, J.D.P. Delgado, R. Veneman, D.W.F. Brilman, Stability of a benzyl amine based CO_2 capture adsorbent in view of regeneration strategies, Ind. Eng. Chem. Res. 56 (2017) 3259–3269, https://doi.org/10.1021/acs.iecr.6b04645.

[37] F. Vidal Vázquez, J. Koponen, V. Ruuskanen, C. Bajamundi, A. Kosonen, P. Simell, J. Ahola, C. Frilund, J. Elfving, M. Reinikainen, N. Heikkinen, J. Kauppinen, P. Piermartini, Power-to-X technology using renewable electricity and carbon dioxide from ambient air: SOLETAIR proof-of-concept and improved process concept, J. CO2 Util. 28 (2018) 235–246, https://doi.org/10.1016/j.jcou.2018.09.026.

[38] H.P. Kläring, C. Hauschild, A. Heißner, B. Bar-Yosef, Model-based control of CO_2 concentration in greenhouses at ambient levels increases cucumber yield, Agric. For. Meteorol. 143 (2007) 208–216, https://doi.org/10.1016/j.agrformet.2006.12.002.

[39] J. Bao, W.-H. Lu, J. Zhao, X.T. Bi, Greenhouses for CO_2 sequestration from atmosphere, Carbon Resour. Convers. 1 (2018) 183–190, https://doi.org/10.1016/j.crcon.2018.08.002.

[40] R. Rodríguez-Mosqueda, J. Rutgers, E.A. Bramer, G. Brem, Low temperature water vapor pressure swing for the regeneration of adsorbents for CO_2 enrichment in greenhouses via direct air capture, J. CO2 Util. 29 (2019) 65–73, https://doi.org/10.1016/j.jcou.2018.11.010.

[41] R. Rodríguez-Mosqueda, E.A. Bramer, G. Brem, CO_2 capture from ambient air using hydrated Na_2CO_2 supported on activated carbon honeycombs with application to CO_2 enrichment in greenhouses, Chem. Eng. Sci. 189 (2018) 114–122, https://doi.org/10.1016/j.ces.2018.05.043.

[42] W. Brilman, L. Garcia Alba, R. Veneman, Capturing atmospheric CO_2 using supported amine sorbents for microalgae cultivation, Biomass Bioenergy 53 (2013) 39–47, https://doi.org/10.1016/j.biombioe.2013.02.042.

[43] Neo-Carbon Food, (2020). http://neocarbonfood.fi/ (accessed March 4, 2020).

[44] J. Wilcox, P.C. Psarras, S. Liguori, Assessment of reasonable opportunities for direct air capture, Environ. Res. Lett. 12 (2017) 065001, , https://doi.org/10.1088/1748-9326/aa6de5.

[45] J. Elfving, C. Bajamundi, J. Kauppinen, Characterization and performance of direct air capture sorbent, Energy Proc. 114 (2017) 6087–6101, https://doi.org/10.1016/j.egypro.2017.03.1746.

[46] M.S. Shafeeyan, W.M.A.W. Daud, A. Shamiri, A review of mathematical modeling of fixed-bed columns for carbon dioxide adsorption, Chem. Eng. Res. Des. 92 (2014) 961–988, https://doi.org/10.1016/j.cherd.2013.08.018.

[47] A.R. Kulkarni, D.S. Sholl, Analysis of equilibrium-based TSA processes for direct capture of CO_2 from air, Ind. Eng. Chem. Res. 51 (2012) 8631–8645, https://doi.org/10.1021/ie300691c.

[48] A. Goeppert, H. Zhang, M. Czaun, R.B. May, G.K.S. Prakash, G.A. Olah, S.R. Narayanan, Easily regenerable solid adsorbents based on polyamines for carbon dioxide capture from the air, ChemSusChem 7 (2014) 1386–1397, https://doi.org/10.1002/cssc.201301114.

[49] A. Sinha, L.A. Darunte, C.W. Jones, M.J. Realff, Y. Kawajiri, Systems design and economic analysis of direct air capture of CO_2 through temperature vacuum swing adsorption using MIL-101(Cr)-PEI-800 and mmen-Mg2(dobpdc) MOF adsorbents, Ind. Eng. Chem. Res. 56 (2017) 750–764, https://doi.org/10.1021/acs.iecr.6b03887.

[50] R. Serna-Guerrero, Y. Belmabkhout, A. Sayari, Influence of regeneration conditions on the cyclic performance of amine-grafted mesoporous silica for CO_2 capture: An experimental and statistical study, Chem. Eng. Sci. 65 (2010) 4166–4172, https://doi.org/10.1016/j.ces.2010.04.029.

[51] M. Parvazinia, S. Garcia, M. Maroto-valer, CO_2 capture by ion exchange resins as amine functionalised adsorbents, Chem. Eng. J. 331 (2018) 335–342, https://doi.org/10.1016/j.cej.2017.08.087.